Journal of Marine Systems 105–108 (2012) 96–105

Contents lists available at SciVerse ScienceDirect

Journal of Marine Systems

journal homepage: www.elsevier.com/locate/jmarsys

Modelling fetch-limited wave growth from an irregular shoreline

Laura Tuomi [a,*], Kimmo K. Kahma [a], Carl Fortelius [b]

[a] Marine Research, Finnish Meteorological Institute, P.O. Box 503, FI-00101 Helsinki, Finland
[b] Meteorological Research, Finnish Meteorological Institute, P.O. Box 503, FI-00101 Helsinki, Finland

ARTICLE INFO

Article history:
Received 10 October 2011
Received in revised form 7 June 2012
Accepted 18 June 2012
Available online 1 July 2012

Keywords:
Wave modelling
WAM
Fetch-limited wave growth
Irregular shoreline
Grid resolution
Re-analysed HIRLAM wind field

ABSTRACT

The wave model WAM was used to study the effect of the grid resolution and the description of an irregular shoreline on modelling of fetch-limited wave growth. Three different methods to compile a grid for a wave model in the case of an irregular shoreline are discussed. Several combinations of shoreline description, grid resolution, and wind field were used to model the effect of the irregularities of the shoreline on fetch-limited wave growth. The modelling confirmed the usual assumption that these effects will rapidly vanish as the distance from the shore increases. However, close to the shoreline the differences between the modelled values of significant wave height were relatively large. The modelled spectral wave parameters were compared against wave measurements made in the Bothnian Sea in 1976. None of the combinations was able accurately to predict the measured wave growth. Close to the shoreline the modelled wave energy and peak period grew too fast, and further offshore the modelled wave energy was underestimated. Close to the shoreline the most accurate results were obtained when a high-resolution grid of 0.25 nmi was used together with a re-analysed wind field from the atmospheric model HIRLAM. The effect of grid resolution on the growth rate of the wave energy at short fetch was relatively large.

1. Introduction

In the northern part of the Baltic Sea (Fig. 1) the shoreline is irregular and sheltered by thousands of small islands ranging from a few meters to several kilometres in diameter. On the scale of the Baltic Sea basin the resolution of operational wave model implementations is typically ca. 10 km or slightly smaller (e.g. Soomere et al., 2008), and with such a resolution the shoreline cannot be resolved in full detail. Some features are so small that they cannot be resolved by any grid size possible today. We therefore need to develop methods to approximate the complex shoreline by a simplified grid, which, possibly together with special subroutines in the model, is able to reproduce the essence of the effects of the irregular shoreline.

The fetch-limited wave growth experiment of Kahma (1981) in the Bothnian Sea is one of the experiments where the waves grow from an irregular shoreline. Moreover, it represents an experiment in which the wind conditions were close to ideal: a nearly constant offshore wind was blowing for several days. At the same time it represents, together with the measurements in Lake Ontario of Donelan et al. (1985), the rapid fetch-limited wave growth which is seldom observed in the field. Kahma and Calkoen (1992) found that when waves are growing in a steady or slowly increasing wind this rapid growth is observed.

When third-generation wave models such as WAM (WAMDI, 1988) were developed, the computing power allowed the forecasting centres to run them only in open sea areas with a coarse horizontal resolution. Nowadays the enhanced computational resources make it possible to run the third generation wave models operationally with a much higher resolution both on a global and a regional scale (e.g. Bidlot et al., 2002; Lalbeharry et al., 2009), and to apply them to near-shore areas (e.g. Rogers et al., 2003). The need for high-resolution wave predictions in the near-shore areas has led to the development of specialised wave models such as SWAN (Simulation of Waves Near shore) (Booij et al., 1999) for high-resolution predictions in shallow waters. In addition, several improvements have been made to the existing third-generation models in order for them to perform better in near-shore areas (e.g. Hersbach and Janssen, 1999; Monbaliu et al., 2000).

In the Baltic Sea as well as in other relatively small semi-enclosed or enclosed basins the sea state is quite often dominated by a wind sea, and in high wind situations the wave growth is often also fetch-limited. The near-shore high-resolution applications, such as wave modelling at harbour entrances, and the calculations needed for the construction of offshore structures, require that waves close to the shoreline are well predicted. In addition, the combination of the locally generated wave field with the offshore wave field approaching the shoreline needs to be modelled accurately.

The seasonally ice-covered seas form a special case for the fetch-limited wave growth. The ice field can contain open sea areas that vary in shape and size, forming a possibility for fetch-limited

* Corresponding author. Tel.: +358 408617967.
E-mail address: laura.tuomi@fmi.fi (L. Tuomi).

0924-7963/$ – see front matter © 2012 Elsevier B.V. All rights reserved.
doi:10.1016/j.jmarsys.2012.06.004

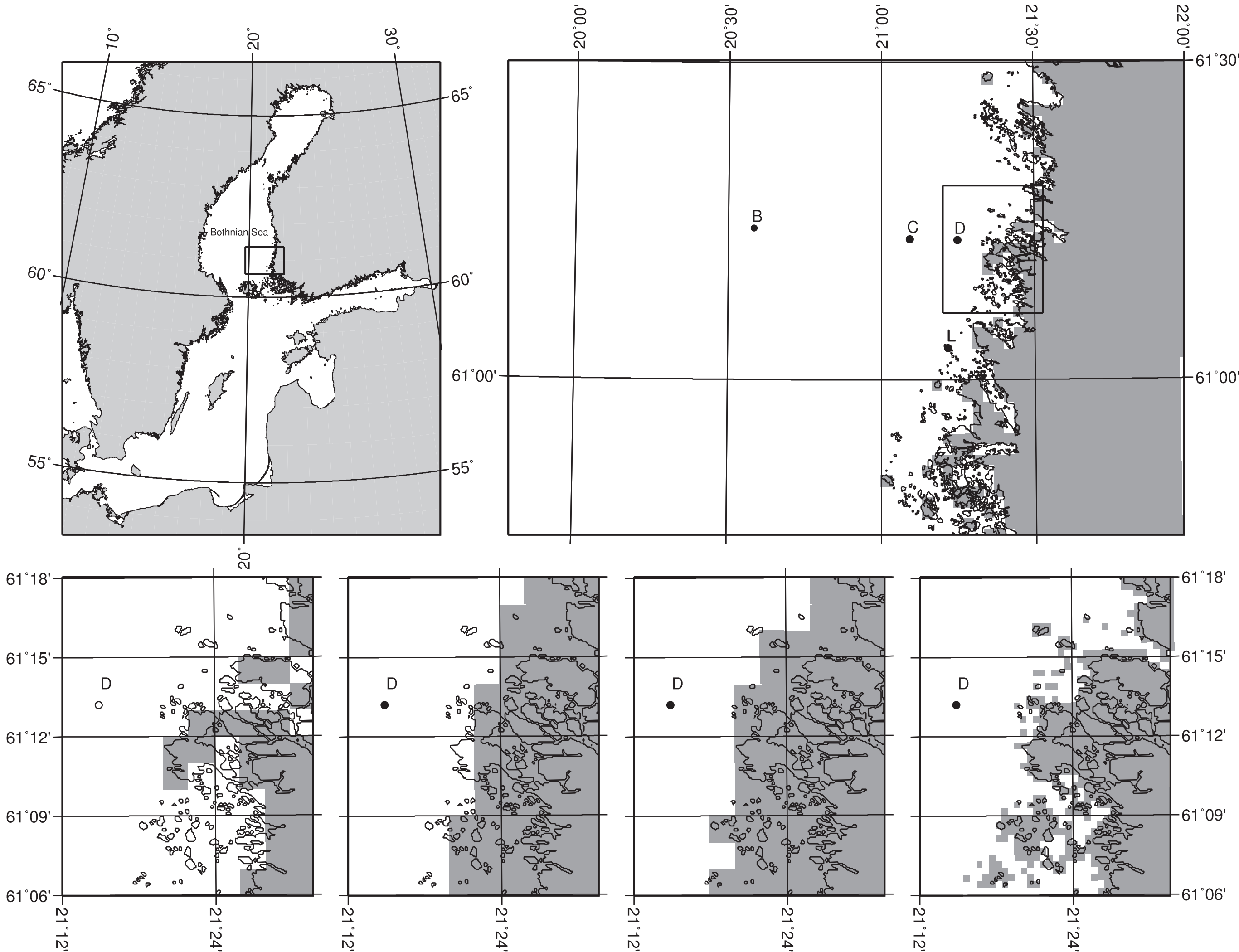

Fig. 1. The Baltic Sea and the location of the sub-basin Bothnian Sea are shown on the upper left panel. On the upper right, the modelling area with land sea distribution from IOW topography (1 nmi resolution, land points with grey colour). Three different shoreline definitions with 1 nmi resolution: IOW topography (IOW_1nmi, on the left), the straight line approximation (STRL_1nmi, second from the left), the shoreline approximated by the FIMR method based on IOW topography and information from nautical charts (FIMR_1nmi, third from the left). FIMR method with 0.25 nmi resolution (FIMR_0.25nmi on the right). Location of wave buoys B, C and D and wind measurement site at Laitakari (L) are shown in the upper right panel.

conditions in areas that during other seasons are in the middle of an open sea. In such cases the fetch-limited conditions need to be accurately modelled also in the case when the used resolution is coarse compared to the size of the area, and the wind speed can be considerably higher than close to the shoreline.

WAM has been used in operational wave forecasting in Finland since 2001, first at the Finnish Institute of Marine Research (FIMR), and since 2009, after the closing down of FIMR, at the Finnish Meteorological Institute (FMI). The accuracy of the open sea wave forecasts and hindcasts has been found sufficient (e.g. Tuomi, 2008; Tuomi et al., 2011). To the knowledge of the authors there are no high-resolution coastal wave model applications implemented in archipelago areas of the northern Baltic Sea for operational purposes. The high-resolution applications of WAM have been found to perform sufficiently well in small basins by e.g. Lalbeharry et al. (2009) in a study including three different models, namely WAM cycle 4.5, SWAM and the K-model implemented and run in Lake Erie. All of these models predicted the wave field with reasonable accuracy, but WAM had the highest accuracy in predicting significant wave height and wave period.

In this paper we study the use of the WAM model in predicting fetch-limited wave growth with emphasis on high-resolution near-shore applications. We present a modelling case study in the Bothnian Sea and compare the results with the experiment made in the area in 1976 (Kahma, 1981). We introduce three different methods to describe the irregularities of the shoreline in a wave model grid, and we study the effect of these on fetch-limited wave growth both near the shore, and further offshore. The differences in the modelled wave parameters are studied both with a constant wind approximation and with a re-analysed wind field, generated using the weather prediction system HIRLAM. The modelled growth of wave energy and peak period is compared with the measurements, and the inaccuracies in the modelled parameters are further studied by an ideal test case of fetch-limited wave growth.

2. Modelling fetch-limited wave growth in the Bothnian Sea

2.1. Definition of the shoreline for the wave model grid

In the northern part of the Baltic Sea the shoreline is sheltered by islands ranging from a few meters to tens of kilometres in diameter. Definition of the shoreline for the wave model grid in cases like this is not trivial. The existing global and regional ocean bottom topographies, such as ETOPO2 (http://www.ngdc.noaa.gov/mgg/global/etopo2.html) or the topography of the Baltic Sea by the Leibniz Institute for Baltic Sea Research Warnemünde (IOW, Seifert et al., 2001) describe the general properties of the coastline (e.g. Fig. 1). However, in the northern

Baltic Sea the irregular shoreline, the archipelago, and shoals make the definition of mean water depth at 1 nautical mile (ca. 1.852 km) resolution (which is the resolution of IOW topography) challenging. Typically areas covered with small islands (as in Fig. 1 in the southern part of the small maps) are defined as sea points in IOW topography. This kind of archipelago will severely affect both fetch-limited wave growth and the propagation of waves from the open sea to the shore, and it needs to be taken into account in the wave model grid. Also in the global shoreline databases, such as GSHHS (A Global Self-consistent, Hierarchical, High-resolution Shoreline Database, Wessel and Smith, 1996), the shoreline of the northern Baltic Sea is not presented in full detail.

To give a better estimate for the fetch, one possibility is to approximate the average fetch of the irregular shoreline by a least-squares fit to the shoreline of the islands or mainland, exposed to the open sea. This approximation was made in Kahma (1981). When implementing the wave model WAM at the former FIMR a better approximation of the shoreline was developed by modifying the grid manually so that areas sufficiently covered by small islands and shoals were coded as land. Hereafter we refer to this method as the FIMR method; at present this work is continued in the Marine Research Unit at FMI. Data from the available topographies was adjusted using information from coastal nautical charts. The method is somewhat subjective, but as a guideline, grid points that have transparency smaller than 40 % are coded as land.

The study area is along the eastern coast of the Gulf of Bothnia in the Baltic Sea (Fig. 1). Four different grids were constructed with the three different methods to define the shoreline for the wave model:

1. IOW_1nmi: One nautical mile (1 nmi) resolution Baltic Sea topography created by IOW (Seifert et al., 2001), with no changes to the shoreline structure. 1 nmi corresponds to 1.852 km both for longitude and latitude in the model grid.
2. STRL_1nmi: The irregular shoreline was approximated by a straight line that estimates the average fetch calculated by a least-squares fit, at a resolution of 1 nmi.
3. FIMR_1nmi: The FIMR method of creating a wave model grid, based on the IOW topography and information from nautical charts to take into account all the small islands, resolution 1 nmi.
4. FIMR_0.25nmi: Same as FIMR_1nmi but with 0.25 nmi (ca. 463 m) resolution for both longitude and latitude.

2.2. Wave modelling with a constant wind field approximation

During offshore winds sufficiently far from the irregular shoreline the waves grow in the same way as from a straight shoreline, provided that the average of the irregular fetch is used (Kahma, 1981). The sensitivity of the growth rate of energy in an ocean wave model to different shoreline definitions was studied by running the wave model WAM cycle 4.5. Compared with WAM cycle 4 (Komen et al., 1994; WAMDI, 1988), in WAM cycle 4.5 several modifications have been included, proposed e.g. by Monbaliu et al. (2000), and a source term for depth-induced wave breaking (Battjes and Janssen, 1978) has been implemented. WAM is based on an energy balance equation that equates the development of the two-dimensional wave spectrum $F(f,\theta)$ to the sum of four terms: the wind input (S_{in}), the wave dissipation due to white-capping (S_{ds}), the bottom friction (S_{bt}), and the discrete approximation of weak nonlinear wave-wave interactions (S_{nl}):

$$\frac{\partial F(f,\theta)}{\partial t} + c_g \cdot \nabla F(f,\theta) = S_{in} + S_{ds} + S_{bt} + S_{nl} \tag{1}$$

where θ is the direction, f the frequency, and c_g is the group velocity.

The wave spectra were modelled with 24 directions and 40 frequencies (ranging from 0.042 to 1.719 Hz). WAM was run in its shallow water mode with depth refraction, even though in the area of interest the bottom depth is sufficient that the waves growing offshore can be regarded as deep water waves. Depth-induced wave breaking was not used, however. We ran WAM with constant offshore winds of 14 m/s speed with the four grids specified in Section 2.1. The wind speed used in this study matches the marine wind estimates made by expert meteorologists at FMI in October 13–15 1976.

The measurement dataset from the Bothnian Sea comprises wave measurements from wave buoys located at 7 km (D), 16 km (C) and 45 km (B) offshore (Fig. 1). Data were collected from the wave buoys every 3 hours. In addition to wave measurements, wind measurements were made at a small flat islet Laitakari, located approximately 7 km offshore; far enough from the mainland and nearby islands so that the wind speed represents the wind over water at the outer archipelago. The wind speed at Laitakari is considerably higher than that at the nearest measuring place on the mainland, and comparison against measurements onboard R/V Aranda several kilometres further offshore from Laitakari did not reveal a bias (Kahma, 1981; Kahma and Leppäranta, 1981). A more detailed description of the dataset can be found in Kahma (1981).

The modelled growth of significant wave height with fetch is presented from two locations, one close to the area in which the wave measurements were made in 1976 (Fig. 2a), and the other from further south representing an area where in addition to the irregular shoreline there are many small islands and shoals close to the shoreline (Fig. 2b). For both locations the differences in the modelled significant wave height with different grids were relatively large close to the shoreline. When the significant wave height was less than 1.5 m the differences were up to 0.2 m in the profile located close to the measurement area, and up to 0.5 m in the profile representing an area where the shoreline is screened by small islands. With increasing fetch the differences are reduced and disappear at 40 km distance from the average shoreline. With longer fetches (of over 40 km) the higher resolution (0.25 nmi) grid gives slightly smaller values, up to 0.05 m, of significant wave height than the coarser resolution (1 nmi) grids.

With the IOW_1nmi grid at short fetch the growth rate of wave energy differs from the ones calculated with the other grids. In the IOW_1nmi grid at grid points close to the shoreline (typically coded as land points in the other grids) the mean water depth is affected by shoals and small islands in the area of the grid point: it is typically between 1 and 4 m. Therefore, at short fetches the growth of wave energy calculated with the IOW_1nmi grid is affected by the shallow water, whereas in other grids the water at the first grid points is deep enough for the waves to be considered as deep water waves in a case of fetch-limited wave growth.

The values of measured significant wave height during the offshore wind event on 13 – 15 October 1976 were 1.42 m–2.48 m at buoy B, 0.92 m–1.27 m at buoy C , and 0.62 m–0.85 m at buoy D. At the location of buoys D and C the constant wind approximation with 14 m/s wind speed (Fig. 2a) gives a significant wave height greater than any of the buoy measurements. At the location of buoy B the constant wind approximation gives results between the measured values. Considering that a wave model forced by a wind field constant in space and time will only give one answer when run until steady state, whereas the measurements from 1976 show that there is variability in the wind and wave field, a perfect match to the measured growth of wave energy can hardly be expected. The measured wind speed at Laitakari (located 7 km offshore) was lower than the marine wind estimates by FMI duty forecasters. The difference between the marine wind estimate and the measurement at Laitakari was typically 2–3 m/s. A test using the measured winds at Laitakari to run the wave model showed that the significant wave height close to the shoreline dropped approximately by 0.5 m, and thus using Laitakari winds for the forcing gave a better estimate of the significant wave height close to the shoreline. However, with Laitakari wind forcing the wave energy was significantly underestimated at the grid points further offshore.

Although with a constant wind field approximation one cannot expect a perfect match with the measured values, it is a reasonable way to study the differences in fetch-limited wave growth between

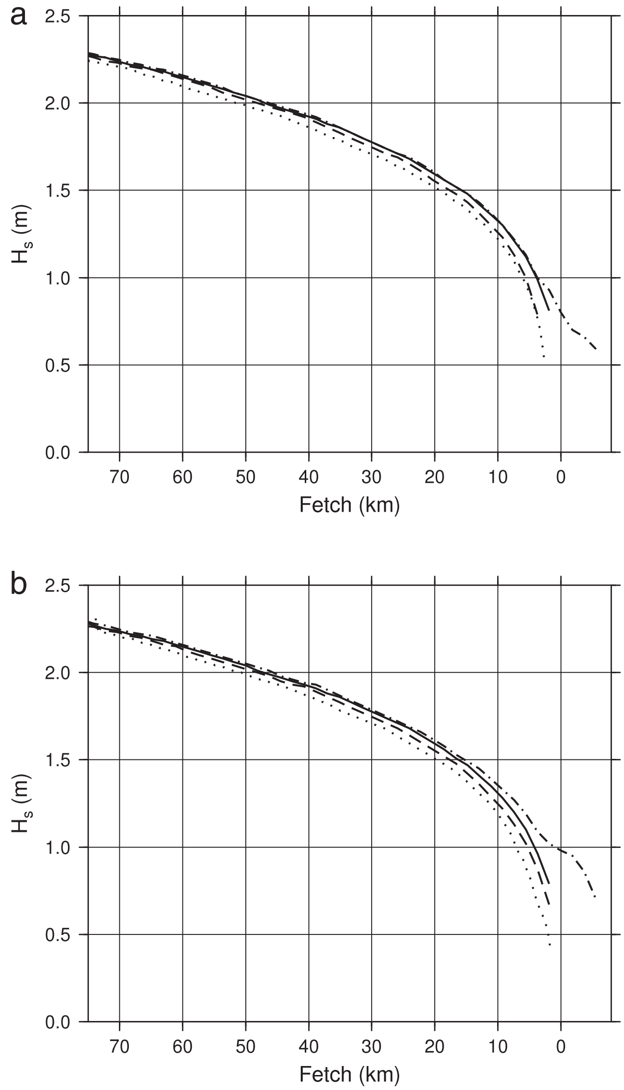

Fig. 2. Fetch-limited growth modelled using three different shoreline approximations. IOW_1nmi (dot-dashed), STRL_1nmi (solid), FIMR_1nmi (dashed) and FIMR_0.25nmi (dotted). Reference approximation for zero fetch in this fig. is the straight line approximation. Negative fetch for the IOW_1nmi means that those grid points are further inland compared to the straight line approximation. In panel a) profile along latitude 61° 13.5′ N and in panel b) profile along latitude 61° 7.5′ N.

the grids. Weather prediction models typically have resolutions coarser than what is used for the wave model in this study. Since the different wave model grids handle the shoreline differently, the values of the interpolated wind speed used at short fetch would also differ. The grids that have points further inland are more likely to use lower wind speeds at short fetch than the grids in which the land-sea boundary is further offshore.

As long as the irregularities are small compared with the distance from the shore, the definition of the shoreline in model grids having the same resolution seems irrelevant. However, when the wave model is used to describe the wave fields in the near-shore areas, the definition of the shoreline becomes important. The effect of grid resolution on the growth of wave energy with fetch will be further discussed later in this paper.

2.3. The re-analysed wind field

In the original analyses of the 1976 Bothnian Sea wave measurements, a constant wind field approximation was used based on the measured data at Laitakari, and the marine wind estimates by FMI (Kahma, 1981). Nowadays more sophisticated tools are available for the reanalysis of the wind field. The reanalysis of global wind fields, such as ERA-40 by the European Center of Medium Range Weather Forecasting (ECMWF) (e.g. Uppala et al., 2005) and NCEP/NCAR by the National Centers for Environmental Prediction (NCEP) and National Center for Atmospheric Research (NCAR) (e.g. Kistler et al., 2001), have provided a tool for wave climate studies, e.g. for validation of current wave prediction models against the field observations that were used as the basis in formulating the physics of the third-generation wave models. However, these reanalyses have too coarse a resolution for wave studies in the Baltic Sea. E.g. Tisler et al. (2007) have shown that in the Baltic Sea the higher resolution and thereby a more accurate description of the land-sea distribution improves the accuracy of the forecast wind field in the coastal areas. Also the spatial variability of the wind field close to the shoreline and inside the archipelago, and for instance sea-breeze circulations, can be better described by high resolution atmospheric models (Savijärvi et al., 2005).

We made the re-analysis of the Bothnian Sea 1976 wind field using the HIRLAM (http://hirlam.org) limited area numerical weather prediction system. HIRLAM was nested into the global ERA-40 analyses, and run in data assimilation mode, producing series of hourly a posteriori forecasts starting daily at 00, 06, 12, and 18 UTC. The meteorological observations were extracted from the ERA-40 archive. We used HIRLAM version 7.1, released in 2007. In our configuration, the HIRLAM domain covers north-western Europe from the British Isles to the Urals. There are 486 by 360 grid-points with a spacing of approximately 7.5 km, and 60 vertical levels. Although the horizontal resolution is rather coarse considering the small-scale features of the northern Baltic Sea shoreline, we found this resolution sufficient to yield an adequate wind forcing in the presence of the land-sea distribution in the area of the measurements made in 1976.

To analyse the accuracy of the HIRLAM wind field in the Bothnian Sea, the modelled wind speed and direction at 10 m height, available at 1 hour intervals, were compared to the 15-minute averages from Laitakari measurements at the same height for the period October 13–15, 1976 (Fig. 3), which is roughly the period used in the original analyses of the wave data by Kahma (1981). During this period an offshore wind was blowing (Fig. 4) and by the measurements at Laitakari the variations in the wind speed were relatively small. Laitakari is located between HIRLAM grid points. Instead of interpolating the HIRLAM wind speed to the Laitakari point, we chose to compare the HIRLAM winds from the two closest points. In both of the HIRLAM grid points, the fraction of land is zero: one of the grid points is the first sea point next to land and the other is the second offshore grid point. At the grid point closer to the shoreline, HIRLAM underestimates the wind speed compared to Laitakari measurements (bias = -1.1 m/s), while at the more offshore grid point the speed is slightly overestimated (bias = 0.2 m/s) (Fig. 3). The HIRLAM wind direction is turned clockwise compared to the measurement in almost all the cases at both HIRLAM grid points (bias = 9 degrees for the grid point closer to the shoreline and bias = 11 degrees for the other grid point). Downwind of the shoreline, the modelled wind shows a typical clockwise turning of about 15 degrees over a distance of about 70 km (not shown). It appears that the HIRLAM wind speed reasonably well agrees with the measurements at Laitakari, which represents well the local wind over water (Kahma, 1981). The re-analysis of the wind field with HIRLAM indicates that there is more variation in the wind field over the Bothnian Sea than that assumed in the original analysis of the data by Kahma (1981).

2.4. Wave modelling using re-analysed wind fields

We used WAM cycle 4.5 to model the growth of wave energy in fetch-limited conditions in the Bothnian Sea using the re-analysed HIRLAM wind fields as the forcing wind. We ran WAM for the whole Baltic Sea area with a 2 nmi resolution to provide boundary

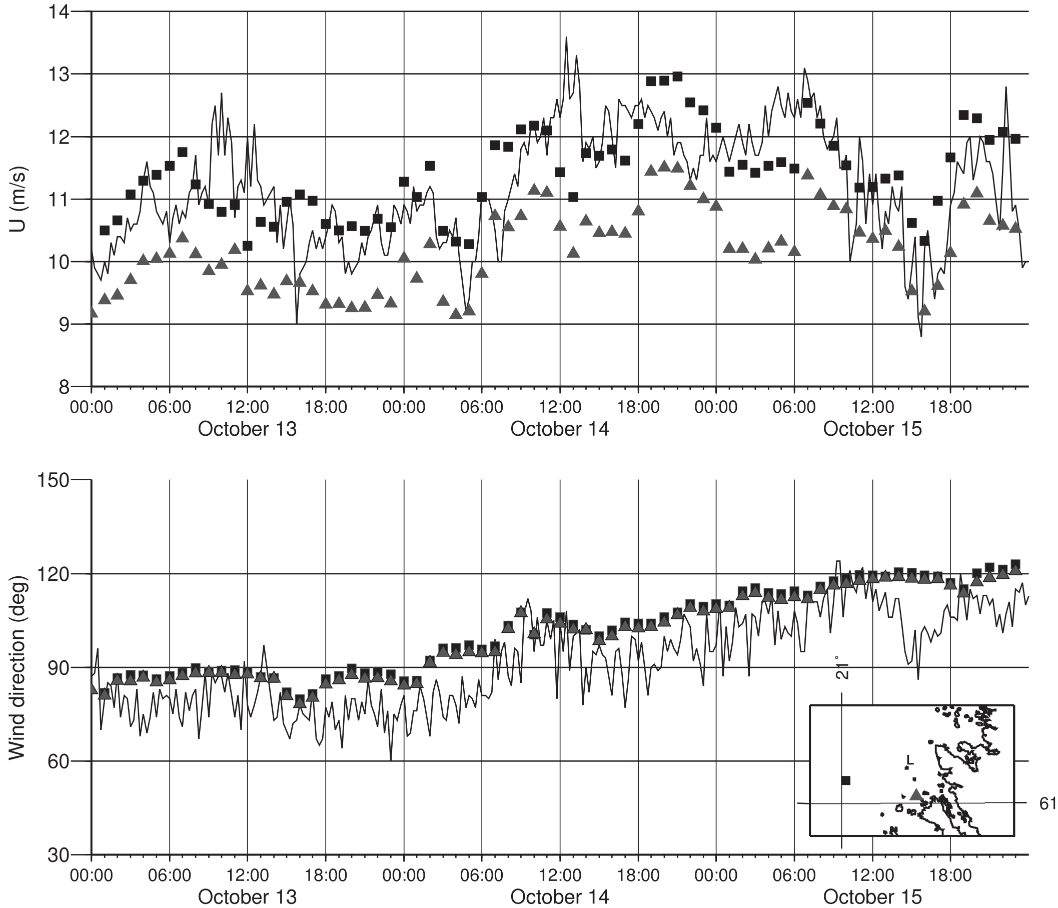

Fig. 3. HIRLAM wind speed and wind direction compared to Laitakari measurements (solid line) on 13–15 October 1976 (comparison against the two closest HIRLAM points (black squares and triangles). Location of the HIRLAM points (square and triangle) and Laitakari (islet marked with L) shown in the map on the lower right corner.

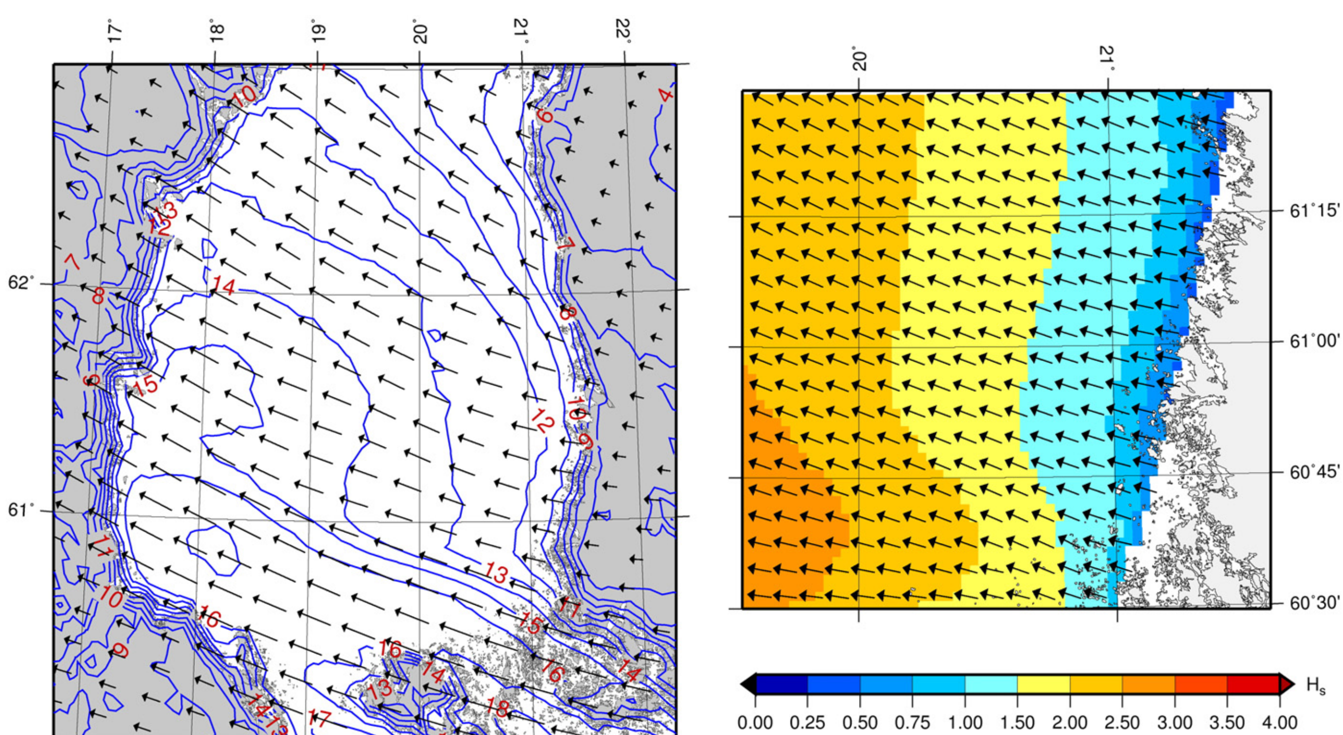

Fig. 4. Modelled wind field (on the left, wind speed with isolines, wind direction with arrows) and wave field (STRL_1nmi grid, on the right, significant wave height with colour, wave direction with arrows) in the Bothnian Sea on 14 October 12 UTC.

information for the limited area runs. The high-resolution area runs were made with the four grids described in Section 2.1. The wave model setup was the same as that described in Section 2.2.

We compared the modelled significant wave height (H_s) and the peak wave period (T_p) against the measurements from the three wave buoys D, C and B (Figs. 5–7 respectively). The period chosen for the validation was from 13 to 15 October 1976. It falls within the period of the best offshore wind conditions, and it is also the period during which the measured wave spectra mostly had a one-peaked structure.

With all the grids the wave parameters are best predicted at buoy C located 16 km offshore. Biases (modelled vs. measured value) in the significant wave height and peak wave period are given in Table 1. At point D, closest to the shoreline, significant wave height is overestimated with IOW_1nmi and STRL_1nmi grids almost throughout the period in question. FIMR_1nmi and FIMR_0.25nmi predict lower significant wave height at point D than the other grids and it is relatively well represented at the beginning of the period but overestimated at the end of the period in question. At point D the peak period is overestimated by all the grids except for few instances in the middle of the period in question. IOW_1nmi predicts highest values of peak period and FIMR_0.25nmi the lowest. FIMR_0.25nmi grid has the smallest bias in significant wave height and peak period at point D. At point B these parameters are underestimated by all the grids. At this point the differences in the modelled significant wave height and peak period by the different grids are small. The IOW_1nmi and STRL_1nmi have the smallest bias in the significant wave height and peak period at point B. Close to the shoreline the growth of wave energy and peak period was most sensitive to the model resolution and the description of the shoreline. Further offshore the results were less affected by the resolution and the description of the shoreline; point B is at a distance at which the differences in the shoreline description become irrelevant as was shown earlier, and point C is close to the distance where details of the shoreline lose their importance.

The WAM runs differ only in the resolution, and in the description of the shoreline. When a higher resolution grid is used, the modelled peak period and wave energy are lower close to the shoreline and agree better with the measurements. Further offshore, the coarser resolution grids predict slightly higher values of wave energy and peak period, which is in better agreement with the measurements. The shoreline description in grids having the same resolution also affects the modelled parameters close to the shoreline. Further offshore the differences disappear.

Since there were differences between the modelled and measured wind speed, the differences between the wave model results and measurements can also be partly explained by this. To study the effect of the wind field accuracy on the wave predictions, we made a detailed comparison of the wind forcing data against the measurement, choosing a period during which the modelled wind speed and direction were in best agreement with the measurements (Fig. 3). On October 14th the wind direction was modelled with good accuracy at both HIRLAM points, and also the wind speed was in relatively good agreement with the measurements (modelled wind and wave fields on 12 UTC 14 October 1976 are shown in Fig. 4). From this period we compared the measured and modelled 1D spectra (11 UTC 14 October

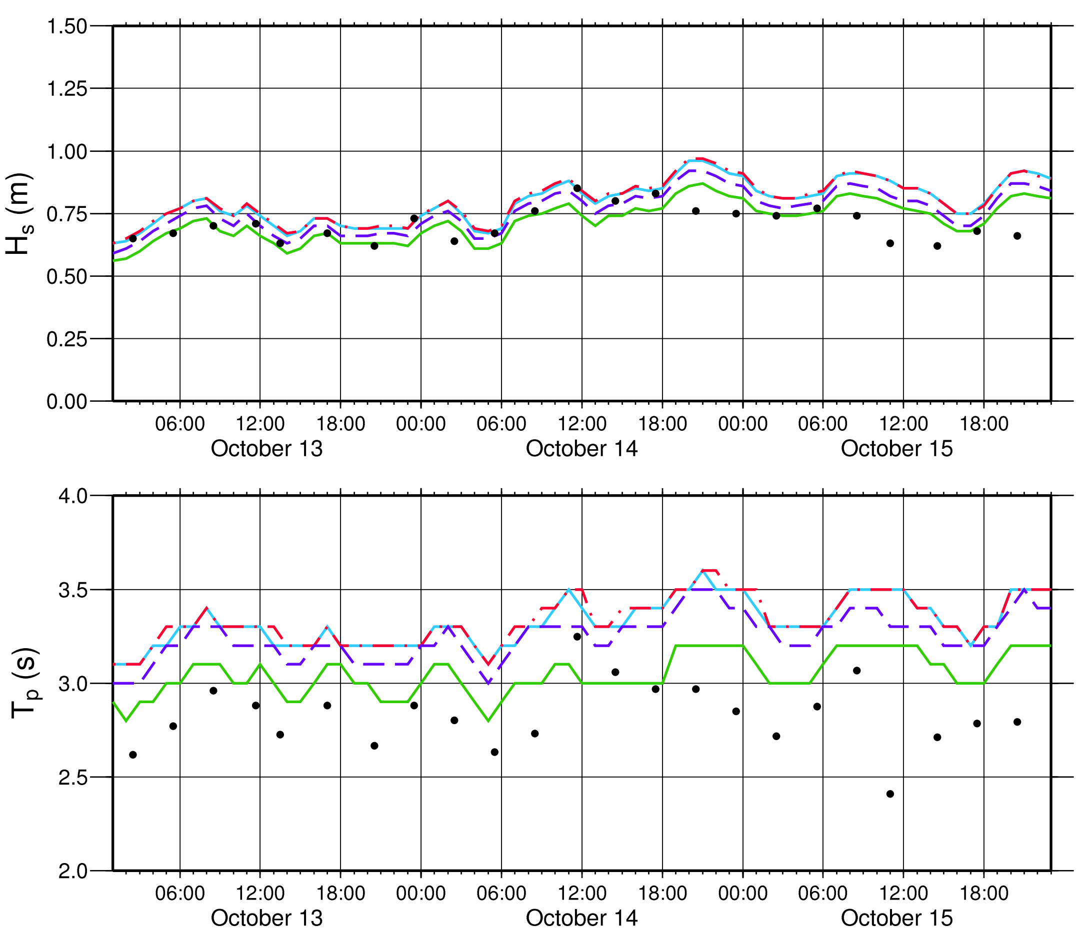

Fig. 5. The modelled significant wave height (upper) and peak period (lower) compared with the measured values from wave buoy D (black dots). IOW_1nmi (red, dot-dashed), STRL_1nmi (light blue, thin solid), FIMR_1nmi (purple, dashed) and FIMR_0.25 nmi (green, solid). Location of buoy D is shown in Fig. 1.

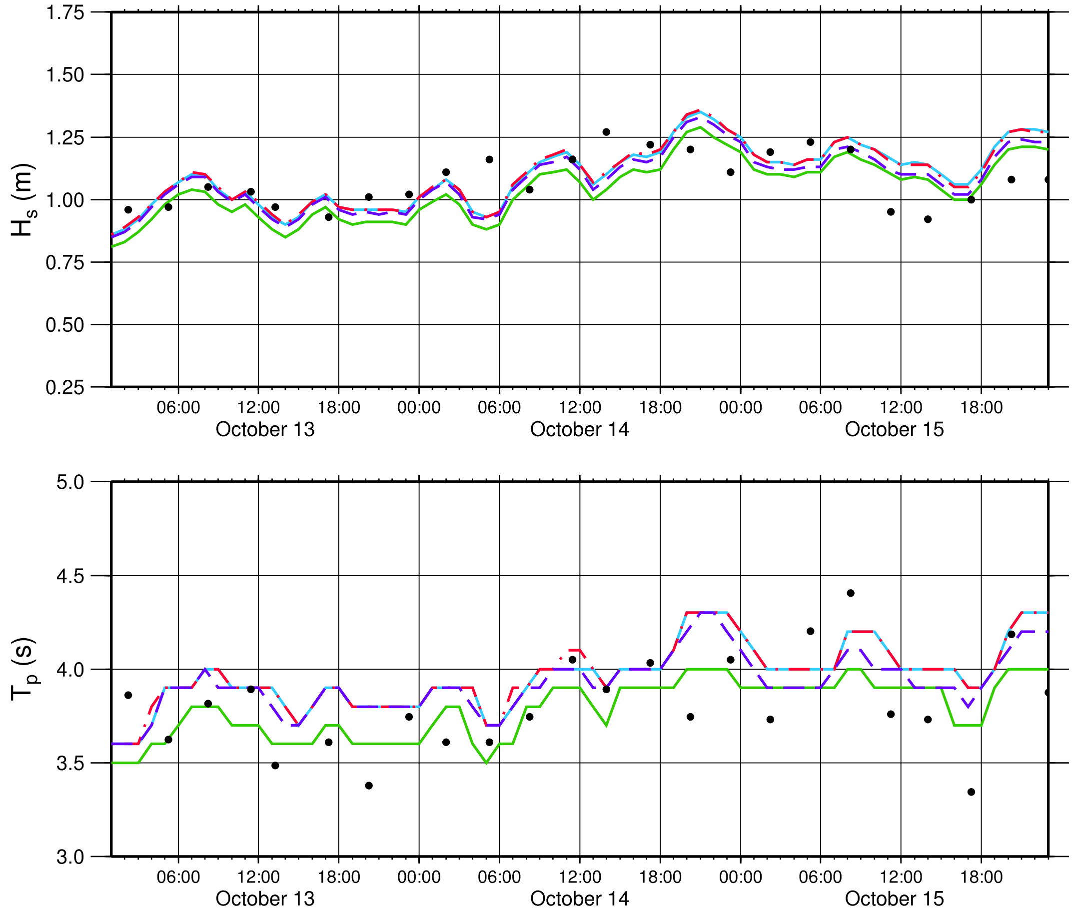

Fig. 6. The modelled significant wave height (upper) and peak period (lower) compared with the measured values from wave buoy C (black dots). IOW_1nmi (red, dot-dashed), STRL_1nmi (light blue, thin solid), FIMR_1nmi (purple, dashed) and FIMR_0.25 nmi (green, solid). Location of buoy C is shown in Fig. 1.

1976). This is approximately six hours after the wind speed had started to increase from 10 m/s, and three hours after the wind speed had reached the value of 12 m/s. At this time the wave spectrum modelled by all the four grids is in good agreement with the measured wave spectrum at points B and C (Fig. 8). At point D (closest to the shoreline) the peak period is overestimated by the 1 nmi grids and the wave energy is underestimated by the 0.25 nmi grid.

No combination of the wave model grid resolution, shoreline description and forcing wind field used in this study was able to predict the spectral wave parameters accurately at all the buoy locations simultaneously.

3. Fetch-limited growth in an ideal case

The fetch limited wave growth in WAM is affected by both the shoreline description in the wave model grid and by the grid resolution as was shown earlier. We therefore wished to study the effect of the resolution on the modelled fetch-limited wave growth separately. We made fetch-limited runs with four grids having 1) 6 nmi (~11.1 km), 2) 1 nmi (~1.852 km), 3) 0.25 nmi (~463 m), and 4) 0.06 nmi (~111 m) resolution, constructed to simulate an infinite shoreline. The model implementation of Section 2 was used except for the frequency range, which was extended to 50 frequencies (up to 4.458 Hz) to ensure that it was reasonable for wave growth at short fetch also for the highest, 0.06 nmi, resolution grid. WAM was run in deep water mode. A constant wind field with a wind speed of 14 m/s was used as forcing for the runs. This corresponds to the marine wind estimate in the 1976 case, and it is the same wind speed that was used earlier in this paper to determine the effect of different shoreline definitions on wave growth. The growth of the significant wave height with fetch in the different resolution grids showed that the higher the resolution, the lower wave energies WAM produces close to the shoreline (Fig. 9). It takes several hundred kilometres before the 1 nmi resolution run reaches the same values of significant wave height as the 6 nmi resolution run.

When analysing the fetch-limited wave growth, we first assumed that the fetch for the first point is the distance to the centre of the preceding land point, but the results do not agree with the measurements: the wave energies WAM produces at the first offshore grid point are higher, and the same applies to following offshore points. Furthermore, the WAM growth curves for energy depend on the grid size.

We tried to match the modelled growth curves of energy with each other by adjusting the fetch of the first grid point. If we add 2 km to the first fetch of 0.25 nmi grid, the growth curves for energy of the 0.06 nmi grid and the 0.25 nmi grid converge at long fetches starting from approximately 15 km fetch. If we further add 5 km to the first fetch of the 1 nmi grid and 25 km to the first fetch of the 6 nmi grid the energy growth curves of all four grids converge when the fetch is over 140 km. We were not able to match the growth rates at short fetches by any adjustments of the fetch of the first point.

Since the additional fetch which is required to make the growth curves to converge is not proportional to the grid size, and the growth at short fetches could not be made to match at all, it appears that the differences cannot be explained just by poorly defined position of the shoreline. Tolman (1992) reported similar dependency between grid resolution and growth rate of wave energy with fetch, and attributed

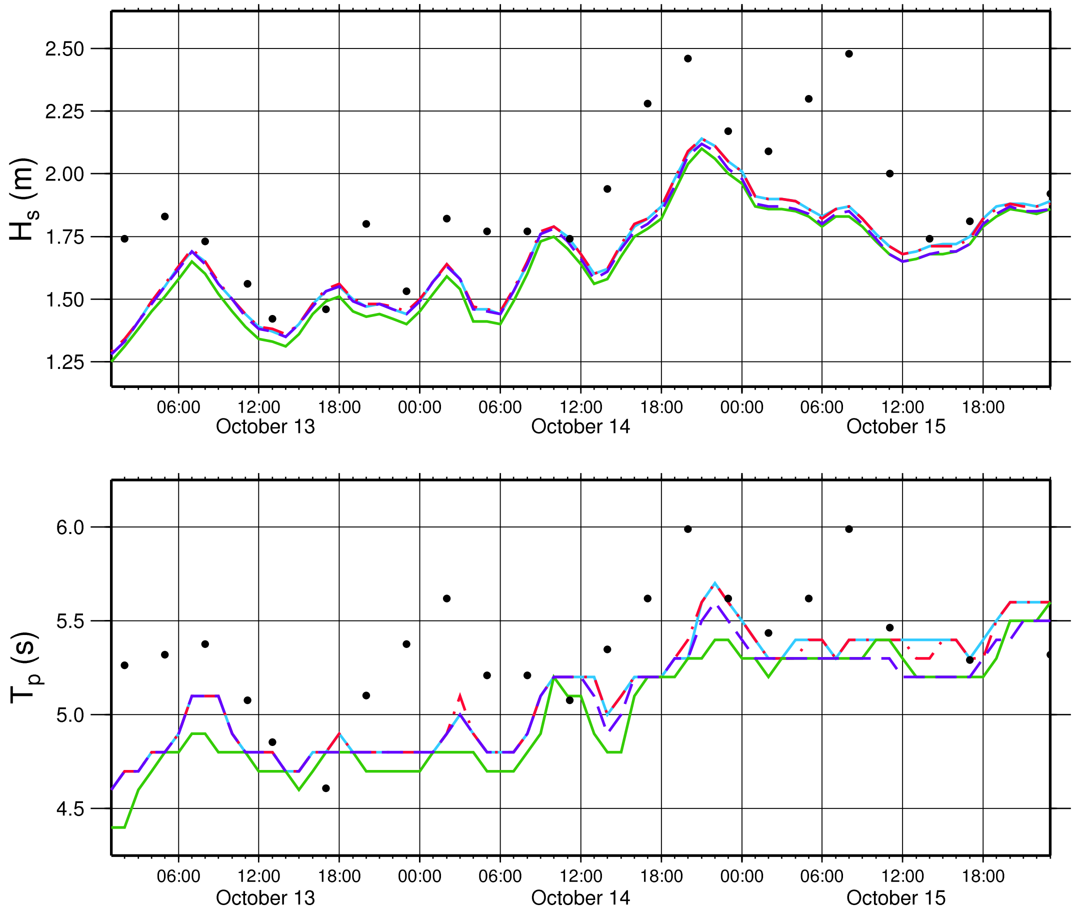

Fig. 7. The modelled significant wave height (upper) and peak period (lower) compared with the measured values from wave buoy B (black dots). IOW_1nmi (red, dot-dashed), STRL_1nmi (light blue, thin solid), FIMR_1nmi (purple, dashed) and FIMR_0.25nmi (green, solid). Location of buoy B is shown in Fig. 1.

it to the numerical propagation error of the first-order upwind scheme used in the WAM model. Also Hersbach and Janssen (1999) found similar departure from the dimensionless growth curves at the beginning of the fetch-limited wave growth after their improvements in the short fetch behaviour of the WAM model. Tolman (1995) showed that the fetch-limited behaviour at short fetch can be improved if a higher-order propagation scheme is used. Implementing a higher-order propagation scheme in the WAM model is planned for testing to see if the overestimation of wave energy at short fetch could be reduced.

The differences in the significant wave height at short fetch between the 1 nmi and 0.25 nmi grids were up to 0.08 m. This accounts for the greater part of the differences we found in the significant wave height in the Bothnian Sea between the 0.25 nmi and 1 nmi grids. However, the definition of the shoreline in the model grid also clearly had an effect on the accuracy of the significant wave height as was shown in Sections 2.2 and 2.4.

The overestimation of wave energy at short fetch may not notably affect the accuracy of model results far from the shore, but it will definitely affect the modelled near-shore fetch-limited growth. Also, this might set the optimal resolution for the wave model higher than is needed for an adequate description of the shoreline. Moreover, this has significant importance also in open sea wave predictions in seasonally ice-covered seas. Inside the ice field there can be open sea areas that vary in shape and size. The ice conditions in the wave models are handled by excluding ice-covered grid points from the calculations. During high wind situations and storms the significant wave height may be severely overestimated in the open sea areas inside the ice field, if the fetch is short and the resolution of the wave model is coarse in comparison with the size of the area.

Recent studies by e.g. van Vledder (2006), van der Westhuysen et al. (2007) and Tsagareli et al. (2010) have suggested several improvements in the source term physics of the wave models. Moreover, Ardhuin et al. (2007), and Romero and Melville (2010) have also shown that modelled wave parameters in fetch-limited conditions and in slanting fetch conditions improve when alternative source terms are used in the wave model. But, for instance, the calculation of the exact non-linear wave-wave interactions is still too time-consuming for operational use when a high resolution is needed.

Table 1
Biases (modelled − measured value) in the modelled significant wave height and peak period at sites B, C and D for all the four different wave model grids.

Significant wave height (H_s)				
BIAS (m)	IOW_1nmi	STRL_1nmi	FIMR_1nmi	FIMR_0.25nmi
Buoy D	0.1	0.09	0.06	0.02
Buoy C	0.02	0.02	0	−0.04
Buoy B	−0.22	−0.22	−0.24	−0.26
Peak wave period (T_p)				
BIAS (s)				
Buoy D	0.51	0.5	0.42	0.22
Buoy C	0.15	0.15	0.11	−0.03
Buoy B	−0.37	−0.37	−0.41	−0.47

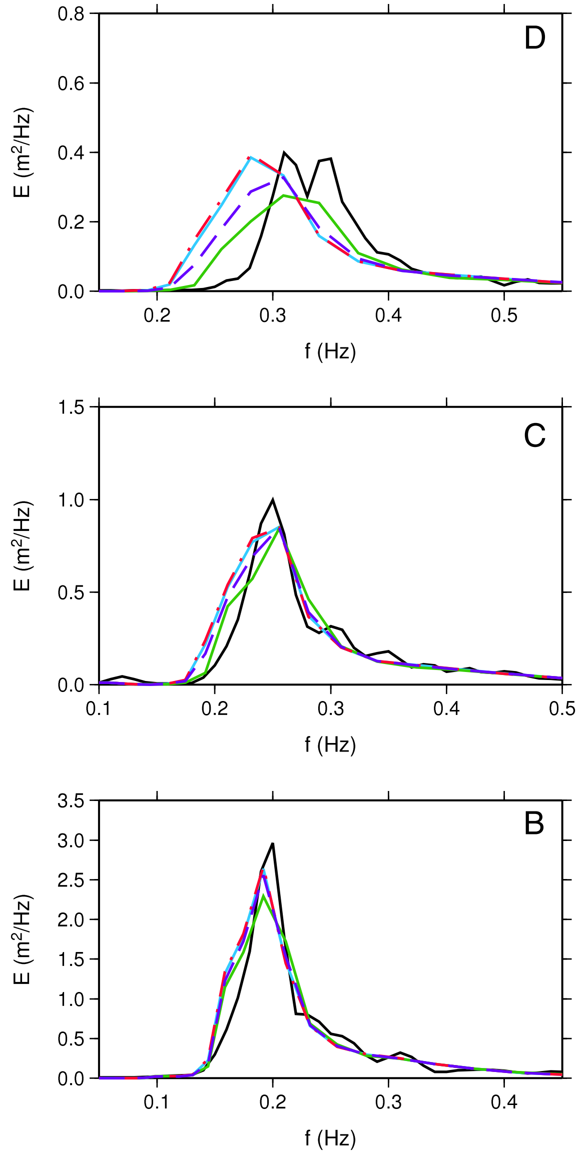

Fig. 8. Measured wave spectra from buoys B, C and D on 11 UTC 14 October 1976 (black, solid) compared to modelled wave spectra. IOW_1nmi (red, dot-dashed), STRL_1nmi (light blue, thin solid), FIMR_1nmi (purple, dashed) and FIMR_0.25 nmi (green, solid).

4. Summary

We studied fetch-limited wave growth with the wave model WAM using several high-resolution grids with different shoreline definitions and forcing wind fields. Wave model results were compared against wave measurements made in the Bothnian Sea in 1976. Defining the shoreline in the model grid when the real shoreline is irregular is not trivial. We used three different methods to construct a wave model grid: 1) straightforward use of existing bathymetry, 2) a straight line approximation of the shoreline, and 3) the FIMR method of modifying available bathymetry with detailed information on small islands and irregularities of the coastline from nautical charts. The resolution used for these grids was 1 nautical mile (ca. 1.852 km). An additional grid with 0.25 nm resolution was constructed using the FIMR method. The three different methods used in this paper showed that with long fetches (of over 40 km) all definitions of the shoreline yielded approximately the same significant wave height. Close to the shoreline the differences between the shoreline descriptions were significant, and in near-shore

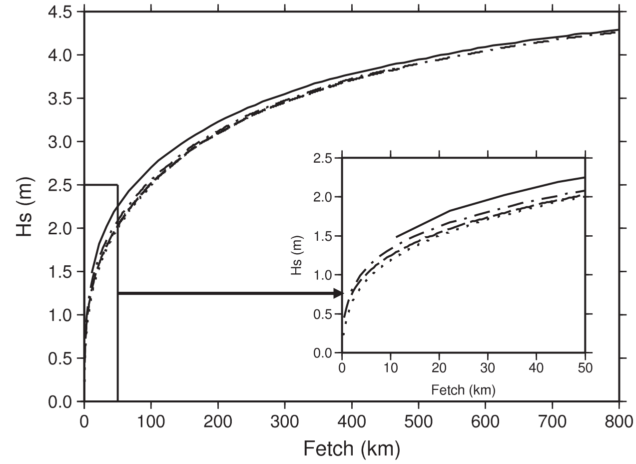

Fig. 9. Growth of significant wave height with fetch calculated with WAM using a grid made to simulate an infinite shoreline. Four different resolutions: 6 nmi (solid), 1 nmi (dot-dashed), 0.25 nmi (dashed) and 0.06 nmi (dotted).

applications special emphasis should be given to the definition of the shoreline in the wave model grid. Available bathymetries and shoreline databases may not be the best tool to estimate the structure of the shoreline. Detailed information on the shoreline from national land use databases, nautical charts, or satellite databases is needed.

Comparison of the modelled significant wave height and peak wave period with measurements made in the Bothnian Sea in 1976 showed that WAM can model the fetch-limited growth of wave energy with sufficient accuracy when the forcing wind field has good quality. During the whole period studied here the best results close to the shoreline were obtained using the re-analysed HIRLAM wind field and a 0.25 nmi resolution grid constructed with the FIMR method. However, close to the shoreline all grids overestimated the peak period. Neither the constant wind field approximation, used when the effects of the shoreline description were studied, nor the re-analysed HIRLAM winds could produce the observed growth of wave energy and peak wave period.

The results from the 1976 case study and runs with ideal grids to simulate an infinite shoreline with constant wind speed suggested that the growth of wave energy and peak period are overestimated at short fetches. The overestimation is reduced when a higher resolution is used.

Acknowledgements

We would like to thank Dr. Heinz Günther from Helmholz-Zentrum Geesthacht for the discussions and comments on fetch-limited growth in the WAM model. The generation of the high-resolution grid for the wave model runs by the FIMR method by Jenni Karjalainen is gratefully acknowledged.

References

Ardhuin, F., Herbers, T.H.C., Watts, K.P., van Vledder, G., Jensen, R., Graber, H.C., 2007. Swell and slanting-fetch effects on wind wave growth. J. Phys. Oceanogr. 37, 908–931.
Battjes, J.A., Janssen, J.P.F.M., 1978. Energy loss and set-up due to breaking of random waves. Proc. 16th Int. Conf. Coastal Eng. ASCE, pp. 569–588.
Bidlot, J.-R., Damian, J., Holmes, P., Wittmann, A., Lalbeharry, R., Chen, H.S., 2002. Intercomparison of the performance of operational ocean wave forecasting systems with buoy data. Wea. Forecasting 17, 287–310.
Booij, N., Ris, R.C., Holthuijsen, L.H., 1999. A third generation wave model for coastal regions 1. Model description and validation. J. Geophys. Res. 104 (C4), 7649–7666.
Donelan, M.A., Hamilton, J., Hui, W.H., 1985. Directional spectra of wind-generated waves. Philos. Trans. R. Soc. London, Ser. A 315, 509–562.
Hersbach, H., Janssen, P.A.E.M., 1999. Improvement of the short-fetch behavior in the Wave Ocean Model (WAM). J. Atmos. Oceanic Technol. 1999 (16), 884–892.
Kahma, K., 1981. A study of the growth of the wave spectrum with fetch. J. Phys. Oceanogr. 11, 1503–1515.

Kahma, K.K., Calkoen, C.J., 1992. Reconciling discrepancies in the observed growth of wind-generated waves. J. Phys. Oceanogr. 22, 1389–1405.
Kahma, K., Leppäranta, M., 1981. On errors in wind speed observations on R/V Aranda. Geophysica 17, 155–165.
Kistler, R., Kalnay, E., Collins, W., Saha, S., White, G., Woollen, J., Chelliah, M., Ebisuzaki, W., Kanamitsu, M., Kousky, V., van den Dool, H., Jenne, R., Fiorino, M., 2001. The NCEP-NCAR 50-year reanalysis: monthly means CD-ROM and documentation. Bull. Am. Meteorol. Soc. 82, 247–268.
Komen, G.J., Cavaleri, L., Donelan, M., Hasselmann, K., Hasselman, S., Janssen, P.A.E.M., 1994. Dynamics and Modelling of Ocean Waves. Cambridge University Press, Cambridge.
Lalbeharry, R., Behrens, A., Guenther, H., Wilson, L., 2009. Matching of coastal and open ocean wave models in a mesoscale application over Lake Erie. Atmosphere-Ocean 47, 184–203.
Monbaliu, J., Padilla-Hernandez, R., Hargreaves, J.C., Carretero Albiach, J.C., Luo, W., Sclavo, M., Gunther, H., 2000. The spectral wave model, WAM, adapted for applications with high spatial resolution. Coastal Eng. 41, 41–62.
Rogers, W.E., Hwang, P.A., Wang, D.W., 2003. Investigation of wave growth and decay in the SWAN model: three regional-scale applications. J. Phys. Oceanogr. 33, 366–389.
Romero, L., Melville, W.K., 2010. Numerical modeling of fetch-limited waves in the Gulf of Tehuantepec. J. Phys. Oceanogr. 40, 466–486.
Savijärvi, H., Niemelä, S., Tisler, P., 2005. Coastal winds and low-level jets: simulations for sea gulfs. Q. J. R. Meteorol. Soc. 131, 625–637.
Seifert, T., Tauber, F., Kayser, B., 2001. A High Resolution Spherical Grid Topography of the Baltic Sea, 2nd edition. Baltic Sea Science Congress, Stockholm, pp. 25–29 (November 2001, Poster #147, www.io-warnemuende.de/iowtopo).
Soomere, T., Behrens, A., Tuomi, L., Nielsen, J.W., 2008. Wave conditions in the Baltic Proper and in the Gulf of Finland during windstorm Gudrun. Nat. Hazard. Earth Syst. Sci. 8, 37–46.
Tisler, P., Gregow, E., Niemelä, S., Savijärvi, H., 2007. Wind field prediction in coastal zone: operational mesoscale model evaluation and simulations with increased horizontal resolution. J. Coast. Res. 23 (3), 721–730.
Tolman, H.L., 1992. Effects of numerics on the physics in a third-generation wind-wave model. J. Phys. Oceanogr. 22, 1095–1111.
Tolman, H.L., 1995. On the selection of propagation schemes for a spectral wind wave model. NWS/NCEP Office Note, 411. (30 pp. + figures).
Tsagareli, K.N., Babanin, A.V., Walker, D.J., Young, I.R., 2010. Numerical investigation of spectral evolution of wind waves. Part I: wind-input source function. J. Phys. Oceanogr. 40, 656–666.
Tuomi, L., 2008. The accuracy of FIMR wave forecasts in 2002–2005. MERI - Report Series of the Finnish Institute of Marine Research, 63, pp. 7–16.
Tuomi, L., Kahma, K.K., Pettersson, H., 2011. Wave hindcast statistics in the seasonally ice-covered Baltic Sea. Boreal Environ. Res. 16, 451–472.
Uppala, S.M., Kållberg, P.W., Simmons, A.J., Andrae, U., Bechtold, V. Da, Costa, Fiorino M., Gibson, J.K., Haseler, J., Hernandez, A., Kelly, G.A., Li, X., Onogi, K., Saarinen, S., Sokka, N., Allan, R.P., Andersson, E., Arpe, K., Balmaseda, M.A., Beljaars, A.C.M., Van De, Berg L., Bidlot, J., Bormann, N., Caires, S., Chevallier, F., Dethof, A., Dragosavac, M., Fisher, M., Fuentes, M., Hagemann, S., Hólm, E., Hoskins, B.J., Isaksen, L., Janssen, P.A.E.M., Jenne, R., McNally, A.P., Mahfouf, J.-F., Morcrette, J.-J., Rayner, N.A., Saunders, R.W., Simon, P., Sterl, A., Trenberth, K.E., Untch, A., Vasiljevic, D., Viterbo, P., Woollen, J., 2005. The ERA-40 re-analysis. Q. J. R. Meteorol. Soc. 131, 2961–3012.
van der Westhuysen, A.J., Zijlema, M., Battjes, J.A., 2007. Nonlinear saturation-based whitecapping dissipation in SWAN for deep and shallow water. Coastal Eng. 54, 151–170.
van Vledder, G.P., 2006. The WRT method for computation of non-linear fourwave interactions in discrete spectral wave models. Coastal Eng. 53, 223–242.
WAMDI, 1988. The WAM model—a third generation ocean wave prediction model. J. Phys. Oceanogr. 18, 1775–1810.
Wessel, P., Smith, W.H.F., 1996. A global self-consistent, hierarchical, high-resolution shoreline database. J. Geophys. Res. 101, 8741–8743.